CHIRALITY 00:000–000 (2008)

Structure Determination of Chiral Sulfoxide in Diastereomeric Bicalutamide Derivatives

WEI LI,[1] DONG JIN HWANG,[1] DIETER CREMER,[2,3]* HYUN JOO,[2] ELFI KRAKA,[2] JUHYUN KIM,[4] CHARLES R. ROSS II,[5] VIET Q. NGUYEN,[1] JAMES T. DALTON,[4] AND DUANE D. MILLER[1]*

[1]*Department of Pharmaceutical Sciences, College of Pharmacy, University of Tennessee Health Science Center, Memphis, Tennessee*
[2]*Department of Chemistry University of Pacific, 3601 Pacific Avenue, Stockton, California*
[3]*Department of Physics, University of Pacific, 3601 Pacific Avenue, Stockton, California*
[4]*Division of Pharmaceutics, The Ohio State University, Columbus, Ohio*
[5]*St. Jude Children's Research Hospital, Memphis, Tennessee*

ABSTRACT We report on the synthesis and investigation of two diastereomers (**5a** and **5b**) of a new bicalutamide analog with an asymmetric carbon atom and a chiral sulfoxide group. These bicalutamide analogs are novel androgen receptor antagonists with biological activities that depend significantly on the configuration of their stereogenic centers. We determined the absolute configuration at the SO center by combining X-ray and NMR measurements with quantum chemical calculations. Since **5a** and **5b** failed to yield satisfactory crystals for X-ray crystal structure determination, analogs **6a** and **6b** differing in only one remote functional group relative to the chiral sulfoxide were synthesized, which yielded satisfactory crystals. X-ray structure determination of **6a** and **6b** provided the absolute configuration at the chiral sulfoxide. Since the structural difference between **5** and **6** is remote from the chiral sulfoxide, the structural assignment was extended from the diastereomers of **6** to those of **5** provisionally. These assignments were verified with the help of measured and DFT-calculated proton and carbon NMR chemical shifts. *Chirality 00:000–000, 2008.*

KEY WORDS: sulfoxide; quantum chemical calculations; NMR; X-ray crystal structure; androgen receptor antagonists

INTRODUCTION

Chiral sulfoxide is an important group in many bioactive molecules, and its absolute configuration often has substantial effects on its biological activity.[1–5] Although many methods have been reported in the literature to determine absolute configuration,[6–12] it is still far from routine to reliably predict the absolute configuration of chiral sulfoxides.[13]

During the synthesis of novel androgen receptors, we obtained two diastereomers of bicalutamide analogs, which showed very different activities. Androgens are of crucial importance in sexual development and function in males and secondary male characteristics such as muscle mass, bone mass, strength, fat distribution, and spermatogenesis.[14–16] The androgen receptor (AR) is an important member of the nuclear superfamily of ligand-activated transcriptional regulators and is responsible for mediating the physiological actions of the androgens testosterone and 5α-dihydrotestosterone.[17,18] Since the discovery of the natural (or endogenous) steroidal androgen testosterone (TES) in the 1930s, a variety of steroidal and nonsteroidal AR ligands have been synthesized and tested. Nonsteroidal AR antagonists such as flutamide,[19] nilutamide,[20,21] and bicalutamide[22,23] are clinically useful prostatic cancer drugs. Of these, the structure of bicalutamide has been the most extensively studied.[24] Bicalutamide and bicalutamide analogs (see Fig. 1) usually have a single chiral center corresponding to an asymmetric carbon atom (*S*-configuration when X = O, NH, and *R*-configuration when X = S, SO_2). It has been demonstrated that the chirality at this center is important for their biological activity against AR.[25–27] When X is –SO–, another chiral center at the sulfur position is introduced, resulting in two diastereomers (for an *R* configuration at the asymmetric carbon: *R, R* or *R, S*). Starting from amides **1** (Fig. 1), we synthesized F1

Contract grant sponsor: College of Pharmacy, University of Tennessee Health Science Center (WL).
Contract grant sponsor: NIH; Contract grant numbers: R01 DK59800, R01 DK065227-04.
Contract grant sponsors: University of the Pacific, American Lebanese Syrian Associated Charities (ALSAC).
Contract grant sponsor: Cancer Center Support CORE; Contract grant number: P30 CA 21765.
*Correspondence to: Dr. Duane D. Miller, Department of Pharmaceutical Sciences, College of Pharmacy, University of Tennessee Health Science Center, Memphis, Tennessee. E-mail: dmiller@utmem.edu or Dr. Dieter Cremer, Department of Chemistry University of Pacific, 3601 Pacific Avenue, Stockton, California. E-mail: dcremer@pacific.edu AQ2
Received for publication 15 August 2007; Accepted 10 June 2008
DOI: 10.1002/chir.20642
Published online in Wiley InterScience (www.interscience.wiley.com).

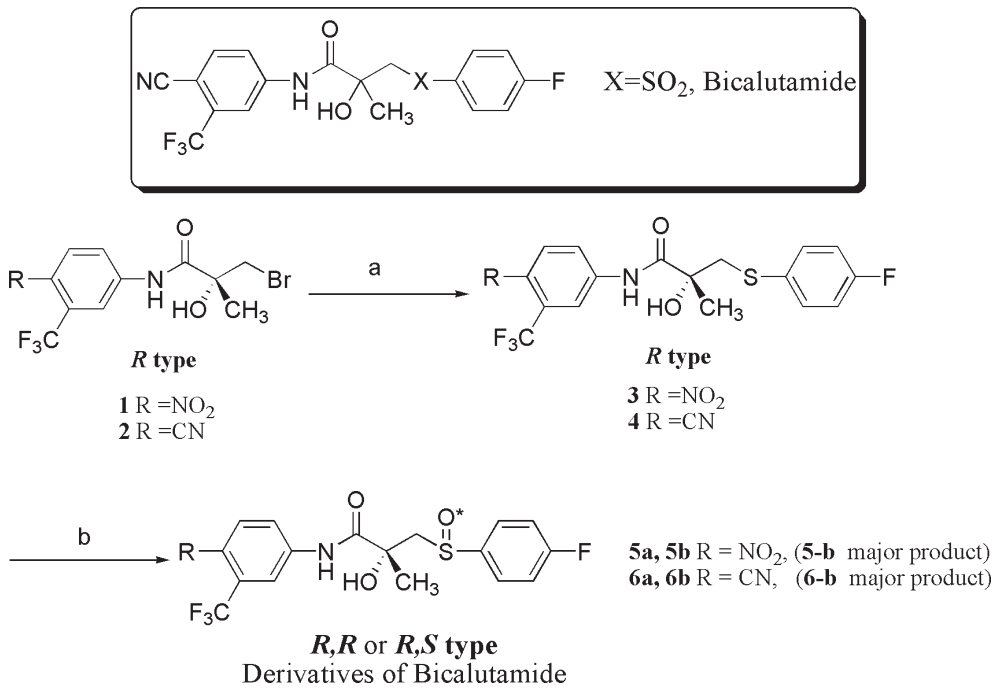

Fig. 1. Structure of bicalutamide, its derivatives, and their synthesis. Reagents and conditions: (a) NaH, THF, 0°C to room temperature, overnight; (b) $NaIO_4$, MeOH, H_2O, room temperature.

bicalutamide analogs **3**. Oxidation of **3** leads to sulfoxides **5**. Interestingly, the diastereomers **5a** and **5b** have very different activity towards AR binding. For the purpose of understanding the biological significance of the absolute configuration of chiral sulfoxide in **5a** and **5b**, we report the structural determination of these two diastereomers by combining X-ray crystal structure studies with NMR measurements and quantum mechanical calculations.

MATERIALS AND METHODS

Synthesis of Sulfoxide-Linked Bicalutamide Derivatives

The synthetic route for compounds (**5** and **6**) is outlined in Figure 1. Briefly, compound **5** and **6** were prepared starting from hydroxybromides **1** and **2**, respectively. For compound **5**, hydroxybromide **1** was synthesized starting from D-proline as a chiral auxiliary.[27] In our coupling reaction, the hydroxybromide was generated to optimized yield (92%) from *R*-3-bromo-2-hydroxy-2-methyl propionic acid[25] with commercially available 4-nitro-3-trifluoromethylaniline by using triethylamine (Et_3N) as a base and THF solvent (Fig. 1). Oxidation of sulfide **3** with sodium periodate produced two diastereomeric sulfoxides in 75% overall yield (27% for **5a**, minor product; 48% for **5b**, major product). Compounds **6a** and **6b** were synthesized with similar yields.

Biological Assay

The AR binding affinity of these compounds was determined using an in vitro competitive radioligand-binding assay with ^{3}H-mibolerone (MIB) as described previously.[28] Briefly, increasing concentrations (10^{-2} nM to 5000 nM) of each ligand were incubated with rat cytosol, ^{3}H-MIB (1 nM), and triamcinolone acetonide (1000 nM) at 4°C for 18 h. At the end of incubation, free and bound ^{3}H-MIB were separated using the hydroxyapatite method. IC_{50} values were determined by computer-fitting the data for each ligand by nonlinear regression analysis. Binding affinities of the ligands were then compared using the calculated K_i values.

NMR Studies

All NMR experiments were performed on a Varian Unity Inova-500 MHz spectrometer equipped with a 5-mm HCN probe (Varian NMR, Palo Alto, CA). The chemical shifts are reported in ppm downfield relative to tetramethylsilane in $CDCl_3$. Temperature was controlled with a general accuracy of ±0.1°C. All NMR data were processed with standard Varian software.

Quantum Chemical Calculations

The diastereomers of **5** and **6** were investigated employing the semiempirical AM1 method[29] for exploratory calculations and density functional theory (DFT) for the actual calculations using in the latter case the B3LYP hybrid functional[30,31] together with Pople's 6-31G(d,p) basis[32,33] for final calculations (509 and 494 basis functions).

For the conformational minima found in this way, harmonic vibrational frequencies were calculated to verify the nature of the stationary points and to determine, besides

energy differences at 0 K, also enthalpy and free energy differences at 298 K. The quantum chemical descriptions of **5** and **6** obtained in this way refer to the gas phase and identify the electronic effects determining their geometry and stability. Since NMR experiments were carried out in $CDCl_3$ solution, we also calculated solvation free energies of the diastereomers of **5** and **6** by employing the conductor-like polarizable continuum model of Barone and coworkers[34] in connection with the dielectric constant of chloroform ($\varepsilon = 4.81$).

For the NMR chemical shift calculations, the DFT-IGLO method of Cremer and Olsson[35,36] was used that is based on a orbital correction factor similar to the one Malkin et al. employed.[37] All calculations were carried out with the program packages COLOGNE07[38] and Gaussian03 (Gaussian, Wallingford, CT, 2004).

X-Ray Crystal Structure Analysis

Despite repeated trials, we were not able to obtain satisfactory single crystals of **5a** and **5b** suitable for X-ray structural analysis. In contrast, satisfactory single crystals from compound **6a** and **6b** were easily generated. Selected crystals were analyzed using X-ray crystallography. Data were collected at 100 K using a Bruker-AXS Proteum CCD area detector and three-circle goniometer. X-rays were supplied by a Nonius FR591 rotating-anode generator using a copper target ($\lambda = 1.54178$ Å) monochromated with Osmic mirrors. Highly redundant data were collected and reduced using SAINT (Bruker AXS, Madison, WI, 1998) and an absorption correction (including a spherical component) applied using SADABS (Bruker AXS, Madison, WI, 2000).

Direct-method structure solution[39] revealed the positions of all nonhydrogen atoms. Structure refinement[40] proceeded smoothly through the application of anisotropic displacement parameters and addition of hydrogen atoms using a riding model. The final structures have been deposited with the Cambridge Crystallographic Data Center (allocated deposition numbers are CCDC 651542 and 651543).

RESULTS AND DISCUSSIONS

Different AR Activities of the Two Diastereomers

Although the **5a** is the minor diastereomer, it is about threefold more potent than **5b** against androgen receptors (**5a**, 71 ± 10 nM; **5b**, 185 ± 95 nM). The chiral center at the carbon atom possesses an *R*-configuration for both epimers; the only difference is the chirality at the sulfoxide group. Clearly the chirality of sulfoxide plays an important role in the binding affinity to androgen receptors. The binding affinity to AR for **6a** and **6b** were lower than that of diastereomers of compound **5** (larger than 770 nM, the upper limit for compounds to be considered inactive).

NMR Analysis

The most significant difference of one dimension ^1H and ^{13}C NMR of **5a** and **5b** is the chemical shift separation of the two protons at C7 next to the chiral sulfoxide (Fig. 2). For **5b**, the coupling constant between the two protons is 13.2 Hz, and the difference in their chemical shifts is 0.5 ppm. The carbon chemical shift for C7 is 65.3 ppm (Fig. 2A). The same methylene group in **5a**, on the other hand, has a proton coupling constant of 13.8 Hz, a carbon chemical shift of 59.2 ppm, and the difference in chemical shifts for the protons at C7 is 0.2 ppm (Fig. 2B). There are also differences in the chemical shifts of other groups, by which **5a** and **5b** can be distinguished. However, we decided to focus our analysis on the C7 methylene group for the following reasons. First, chemical shifts for the protons of the amide and hydroxyl group may have larger variations and uncertainty due to their exchangeable nature. These protons and the protons of the C9 methyl group are also far away from the sulfoxide chiral center. Second, the behaviors of chemical shifts for protons in the aromatic rings are more complicated than that of the methylene protons at C7. The analysis of the chemical shifts of the C7-methylene group offers the simplest and potentially the most reliable method for determining the absolute configuration of the chiral sulfoxide group in **5a** and **5b**.

Although there are some detectable differences in their NOESY spectra, attempts to use NOE-derived distance constraints and molecular dynamics calculations failed to unambiguously determine the structure of **5a** and **5b**. This was mainly due to the large uncertainty of the NOE-derived distance constraints for these relatively flexible molecules and the fact that there are no protons directly at the chiral center.

X-Ray Structural Analysis of Diastereomers 6a and 6b

Diastereomer **6a** (**6b**) shares similar properties (relative yield from synthesis, polarity as indicated by TLC, and chemical shifts of proton NMR) with that of **5a** (**5b**). Since the difference between **5** and **6** is very remote from the chiral sulfoxide center and the corresponding isomers share similar properties, the absolute configuration at the chiral sulfoxide position are expected be the same. Structural determination of **6** is likely to provide information for **5**.

Results from the X-ray analysis of **6a** and **6b** are shown in Figure 3. The structure of **6a** was determined to be C(R)S(R), meaning *R*-configuration at the carbon and *R*-configuration at the sulfur. Correspondingly, the structure of **6b** was found to be C(R)S(S), indicating *S*-configuration at the sulfur position.

Crystals of compound **6a** have $P2_1$ symmetry with two independent molecules in the asymmetric unit. Each of these molecules adopts an L-shaped conformation with the hinge at C8. Both molecules have the leg terminating in the single fluorine pointing along the *b*-axis. However, they differ in the orientation of the leg terminating in CN—one molecule has this leg pointing along the *a*-axis, and the other has this leg pointing along the *c*-axis. The *b*-pointing legs of one molecule type intercalate between pairs of *c*- (or *a*-) pointing legs of molecules of the other type, offering opportunities for edge-center interactions between aromatic rings. There are a number of opportunities for hydrogen-bonding interactions, including intramolecular bonds N1—H···O2 (strengths of 0.08 and 0.11 va-

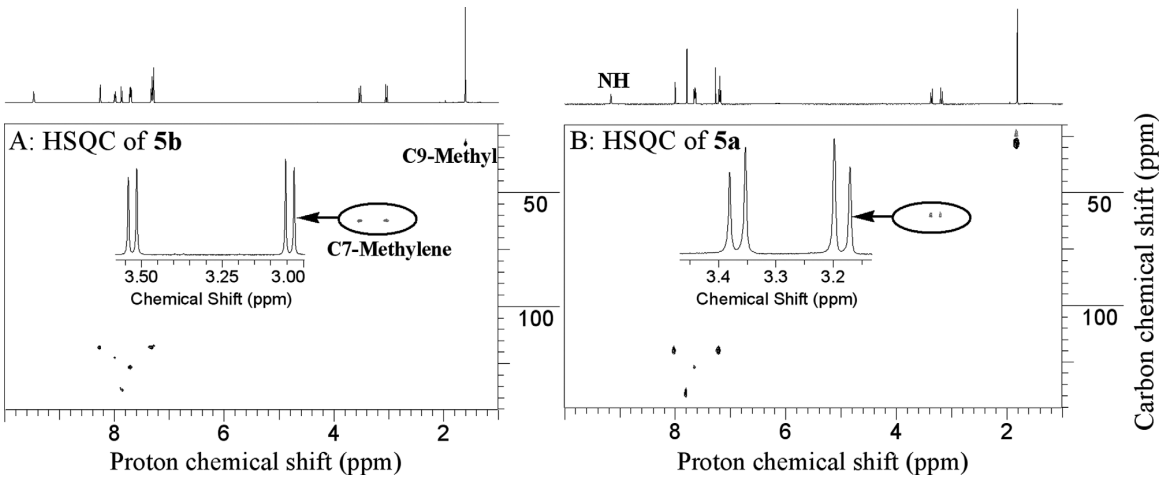

Fig. 2. ^{1}H-^{13}C HSQC spectra for **5a** (**B**) and **5b** (**A**). The corresponding one-dimensional ^{1}H NMR spectra are displayed in the horizontal projection. Group numbering is given in Figure 3. Notice the difference in separation of the chemical shifts in these two diastereomers. [Color figure can be viewed in the online issue, which is available at www.interscience.wiley.com.]

AQ3

lence units, v.u.), and intermolecular bonds N1—H···O1′ (strengths of 0.06 and 0.10 v.u.) and O2—H···O3′ (strengths of 0.08 and 0.12 v.u.). The hydrogen atom on N1 participates in a bifurcated bonding pattern with O2 and O1′.

Crystals of compound **6b** have $P2_12_12_1$ symmetry with one molecule in the asymmetric unit. This molecule is strongly folded with the hinge at C7—the arms of the molecule point roughly along the *c*-axis. A strong intermolecular hydrogen bond O2—H···O1′ (0.16 v.u.) is indicated, and a much weaker (0.04 v.u.) intermolecular hydrogen bond N1—H1···O3′, but no other intermolecular or intramolecular interactions are obvious. The repeated hydrogen-bonding pattern O2′ —H′···O1—S1—C7—C8—O1—O2—H···O1″ forms an infinite spiral linkage with its axis parallel to the *a* crystallographic axis. Successive molecules in this linkage are related by a 2_1(x) symmetry operation.

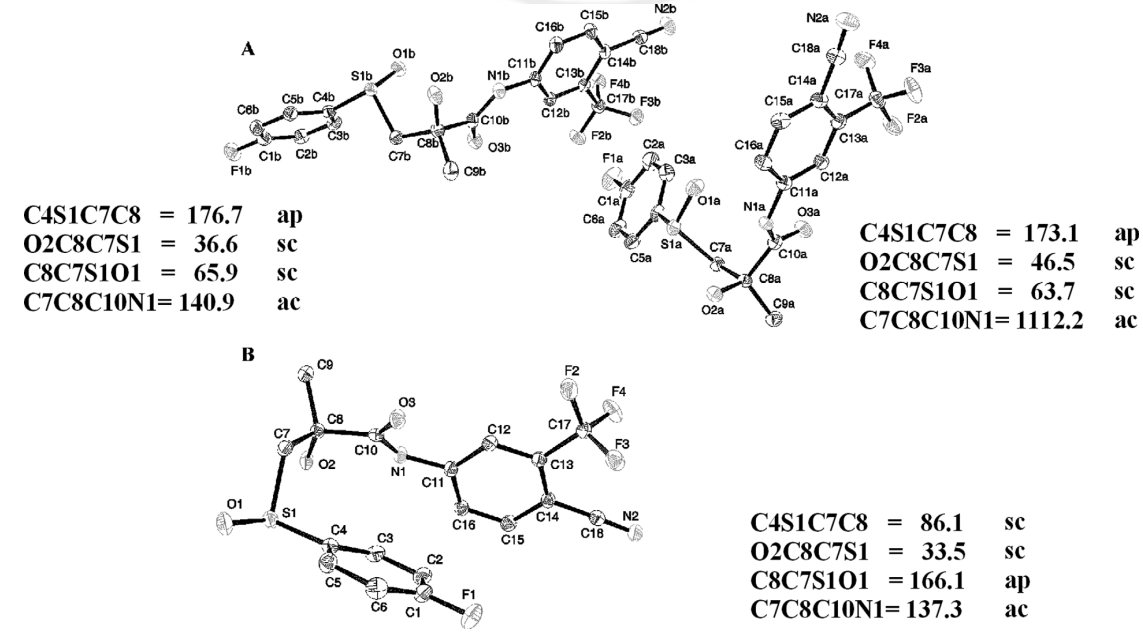

Fig. 3. X-ray structures of **6a** (**A** isomer, C(R)S(R), top) and **6b** (**B** isomer, C(R)S(S), bottom). Conformations are described by measured dihedral angles τ and the short hand notation syn-periplanar (sp: $0 \leq \tau \leq \pm 30^{\circ}$), syn-clinal (sc: $\pm 30 < \tau \leq \pm 90^{\circ}$), anti-clinal (ac: $\pm 90 < \tau \leq \pm 120^{\circ}$), or anti-periplanar (ap: $\pm 120 < \tau \leq \pm 180^{\circ}$). All angles in degrees. ADPs shown at 50% probability. [Color figure can be viewed in the online issue, which is available at www.interscience.wiley.com.]

The packing of molecule **6b** in its crystal structure is modestly (5%) more efficient than that of molecule **6a**.

Therefore, chiral sulfoxide in **5a** should be *R*-configuration and in **5b** should be *S*-configuration. These results are consistent with what we obtained from NMR analysis combined with quantum mechanical calculations (see below).

Quantum Chemical Calculations on 5 and 6

The relative stabilities and the preferred conformation of diastereomers **5a** and **5b** were investigated in $CDCl_3$ ($\epsilon = 4.81$) which is the solvent of the NMR measurements, According to B3LYP/6-31G(d,p) calculations, the relative free energy of the U-form of **5a** shown in Figure 4 is just 1.9 kcal/mol higher than that of the stretched form of **5b,** whereas the stretched form of **5a** (not shown in Fig. 4) is 6.7 kcal/mol higher in energy. We note in this connection that **5b** (**6b**), contrary to **5a** (**6a**) is characterized by a SO···H—O bond of 1.791 Å (Fig. 4) that adds to the stabilization of the diastereomer. This H-bond can also facilitate the oxidation step of **3** (**4**) by periodate.

The calculated ^{1}H and ^{13}C NMR chemical shifts for **5a** and **5b** in their most stable conformations are summarized in Figure 4. On first sight, ^{13}C and ^{1}H NMR chemical shifts of **5a** and **5b** do not differ much from each other (see Fig. 4). Only the C7-methylene group between the chiral centers possesses chemical shifts significantly different in the two diastereomers. For **5a** and **5b**, ^{13}C chemical shifts of $\delta = 47.1$ and 55.7 ppm are calculated (a difference of 8.6 ppm). Experimentally, the chemical shift for this carbon in **5a** (59.2 ppm) is 6.1 ppm downfield relative to that of **5b** (65.3 ppm). The quantum chemical result is consistent with the experimental measurements. There are other, but smaller, differences (e.g., 3 ppm with regard to the chemical shift of the chiral C atom, see Fig. 4), which are probably more difficult to detect. On the basis of these carbon chemical shift differences, **5a** is found to be C(R)S(R) and **5b** to be C(R)S(S) configuration.

The comparison of calculated to measured proton shifts is always difficult because the influence of environmental effects, especially solvent effects, changes the proton spectrum considerably. In addition, exchange of acidic protons in aqueous solution can make the determination of proton shifts experimentally problematic. Nevertheless, one can distinguish certain trends in the proton shifts, which make it possible to identify a given compound with the help of the proton NMR spectrum. Bearing this in mind, we can make the following observations.

In the calculated ^{1}H NMR spectrum, the C7-methylene protons appear both at 3.1 ppm for **5a,** whereas there is a 1-ppm difference between them (3.2 and 2.2 ppm) in the case of **5b** (Fig. 4), which is similar to the shift differences of 0.2 and 0.5 ppm found experimentally. Noteworthy is also that the aromatic protons are somewhat more shielded in the case of **5a** (calculated ^{1}H chemical shifts: 7.2–8.0 ppm, Fig. 4), whereas they are somewhat more deshielded in the case of **5b** (7.4–9.4 ppm). This is also observed experimentally (**5a**: 7.2–8.1 ppm; **5b**: 7.3–8.3 ppm) and can be related to the different conformations of the two diastereomers. The U-conformation of **5a** brings the two phenyl rings in a quasi-stacked position (Fig. 4), which leads to shielding of the ring protons in dependence on their position with regard to the other phenyl ring. This effect is missing in the stretch conformation of **5b**. Taking all information from the proton NMR spectra together we suggest that **5b** corresponds to the C(R)S(S) and **5a** to the C(R)S(R) diastereomer. This is consistent with results from the ^{13}C chemical shift analysis and is further supported by subsequent X-ray crystallographic analysis of **6a** and **6b**.

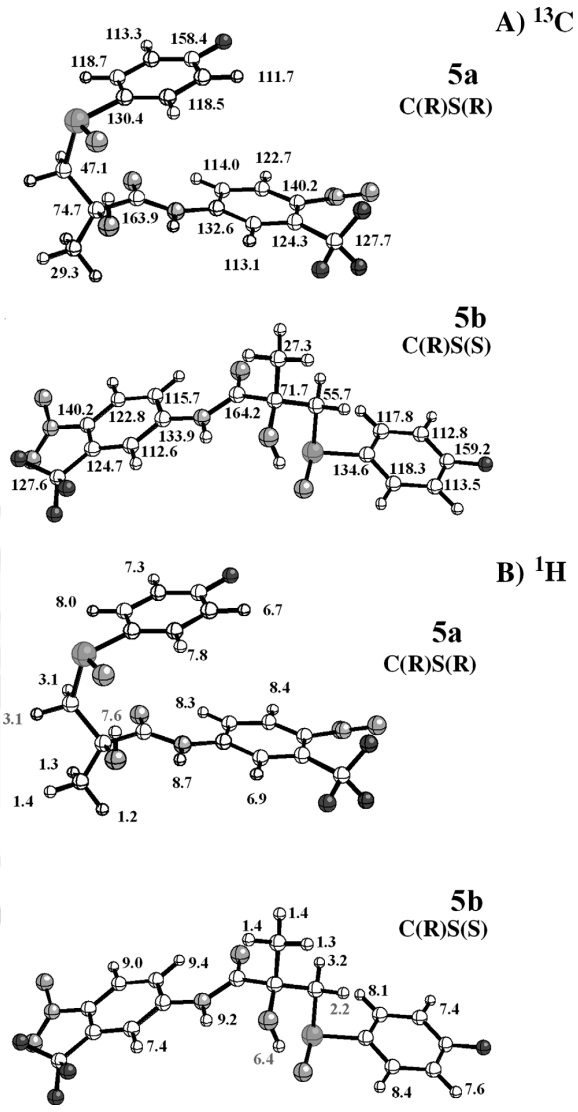

Fig. 4. Most stable conformation of diastereomers **5a** and **5b** according to B3LYP/6-31G(d,p) calculations. (**A**) Carbon and (**B**) proton chemical shifts (in ppm relative to TMS) calculated for a chloroform solution. [Color figure can be viewed in the online issue, which is available at www.interscience.wiley.com.]

In summary, we have determined the structures of two chiral sulfoxide containing bicalutamide analogs by NMR and quantum chemical calculations. This assignment was subsequently confirmed by X-ray crystallography analysis on closely related structures.

ACKNOWLEDGMENT

The authors thank an unknown referee for useful comments concerning the interpretation of the NMR spectra.

LITERATURE CITED

1. Gadepalli RSVS, Rimoldi JM, Fronczek FR, Nillos M, Gan J, Deng X, Rodriguez-Fuentes G, Schlenk D. Synthesis of fenthion sulfoxide and fenoxon sulfoxide enantiomers: effect of sulfur chirality on acetylcholinesterase activity. Chem Res Toxicol 2007;20:257–262.
2. Pellissier H. Use of chiral sulfoxides in asymmetric synthesis. Tetrahedron 2006;62:5559–5601.
3. Bentley R. Role of sulfur chirality in the chemical processes of biology. Chem Soc Rev 2005;34:609–624.
4. Fernandez I, Khiar N. Recent developments in the synthesis and utilization of chiral sulfoxides. Chem Rev (Washington, DC) 2003;103: 3651–3705.
5. Solladie G. Applications of chiral sulfoxides in enantioselective synthesis of diols and total synthesis of natural products. Heteroatom Chem 2002;13:443–452.
6. Donnoli MI, Giorgio E, Superchi S, Rosini C. Circular dichroism spectra and absolute configuration of some aryl methyl sulfoxides. Org Biomol Chem 2003;1:3444–3449.
7. Stephens PJ, Devlin FJ, Cheeseman JR, Frisch MJ, Rosini C. Determination of absolute configuration using optical rotation calculated using density functional theory. Org Lett 2002;4:4595–4598.
8. Devlin FJ, Stephens PJ, Scafato P, Superchi S, Rosini C. Determination of absolute configuration using vibrational circular dichroism spectroscopy: the chiral sulfoxide 1-thiochromanone S-oxide. Chirality 2002;14:400–406.
9. Devlin FJ, Stephens PJ, Scafato P, Superchi S, Rosini C. Conformational analysis using infrared and vibrational circular dichroism spectroscopies: the chiral cyclic sulfoxides 1-thiochroman-4-one S-oxide, 1-thiaindan s-oxide and 1-thiochroman S-oxide. J Phys Chem A 2002; 106:10510–10524.
10. Stephens PJ, Aamouche A, Devlin FJ, Superchi S, Donnoli MI, Rosini C. Determination of absolute configuration using vibrational circular dichroism spectroscopy: the chiral sulfoxide 1-(2-methylnaphthyl) methyl sulfoxide. J Org Chem 2001;66:3671–3677.
11. Donnoli MI, Superchi S, Rosini C. Chromatographic resolution and elution order of alkyl aryl and aryl benzyl sulfoxides on cellulose-based chiral stationary phases. Enantiomer 2000;5:181–188.
12. Yabuuchi T, Kusumi T. NMR Spectroscopic determination of the absolute configuration of chiral sulfoxides via *N*-(methoxyphenylacetyl)sulfoximines. J Am Chem Soc 1999;121:10646–10647.
13. Kusumi T, Ooi T, Ohkubo Y, Yabuuchi T. The modified Mosher's method and the sulfoximine method. Bull Chem Soc Jpn 2006;79:965–980.
14. Chen J, Hwang DJ, Bohl CE, Miller DD, Dalton JT. A selective androgen receptor modulator for hormonal male contraception. J Pharmacol Exp Ther 2005;312:546–553.
15. Matsumoto AM. Effects of chronic testosterone administration in normal men: safety and efficacy of high dosage testosterone and parallel dose-dependent suppression of luteinizing hormone, follicle-stimulating hormone, and sperm production. J Clin Endocrinol Metab 1990;70:282–287.
16. Tucker H, Chesterson GJ. Resolution of the nonsteroidal antiandrogen 4′-cyano-3-[(4-fluorophenyl)sulfonyl]-2-hydroxy-2-methyl-3′-(trifluoromethyl)-propionanilide and the determination of the absolute configuration of the active enantiomer. J Med Chem 1988;31:885–887.
17. Van Dort ME, Robins DM, Wayburn B. Design, synthesis, and pharmacological characterization of 4-[4, 4-dimethyl-3-(4-hydroxybutyl)-5-oxo-2-thioxo-1-imidazolidinyl]- 2-iodobenzonitrile as a high-affinity nonsteroidal androgen receptor ligand. J Med Chem 2000;43:3344–3347.
18. Evans RM. The steroid and thyroid hormone receptor superfamily. Science 1988;240:889–895.
19. Schroder FH, Whelan P, de Reijke TM, Kurth KH, Pavone-Macaluso M, Mattelaer J, van Velthoven RF, Debois M, Collette L. Metastatic prostate cancer treated by flutamide versus cyproterone acetate. Final analysis of the "European Organization for Research and Treatment of Cancer" (EORTC) Protocol 30892. Eur Urol 2004;45:457–464.
20. Kassouf W, Tanguay S, Aprikian AG. Nilutamide as second line hormone therapy for prostate cancer after androgen ablation fails. J Urol 2003;169:1742–1744.
21. Dukes M, Furr BJ, Hughes LR, Tucker H, Woodburn JR. Nonsteroidal progestins and antiprogestins related to flutamide. Steroids 2000;65:725–731.
22. Schellhammer PF, Davis JW. An evaluation of bicalutamide in the treatment of prostate cancer. Clin Prostate Cancer 2004;2:213–219.
23. James KD, Ekwuribe NN. A two step synthesis of the anti-cancer drug (R, S)-bicalutamide Synthesis. Synthesis 2002;7:850–852.
24. Dalton JT, Mukherjee A, Zhu Z, Kirkovsky L, Miller DD. Discovery of nonsteroidal androgens. Biochem Biophys Res Commun 1998;244:1–4.
25. Hwang DJ, Yang J, Xu H, Rakov IM, Mohler ML, Dalton JT, Miller DD. Arylisothiocyanato selective androgen receptor modulators (SARMs) for prostate cancer. Bioorg Med Chem 2006;14:6525–6538.
26. Marhefka CA, Gao W, Chung K, Kim J, He Y, Yin D, Bohl C, Dalton JT, Miller DD. Design, synthesis, and biological characterization of metabolically stable selective androgen receptor modulators. J Med Chem 2004;47:993–998.
27. Kirkovsky L, Mukherjee A, Yin D, Dalton JT, Miller DD. Chiral nonsteroidal affinity ligands for the androgen receptor. I. Bicalutamide analogues bearing electrophilic groups in the B aromatic ring. J Med Chem 2000;43:581–590.
28. Mukherjee A, Kirkovsky LI, Kimura Y, Marvel MM, Miller DD, Dalton JT. Affinity labeling of the androgen receptor with nonsteroidal chemoaffinity ligands. Biochem Pharmacol 1999;58:1259–1267.
29. Dewar MJS, Reynolds CH. An improved set of mndo parameters for sulfur. J Comput Chem 1986;7:140–143.
30. Becke AD. Density-functional thermochemistry. III. The role of exact exchange. J Chem Phys 1993;98:5648–5652.
31. Lee C, Yang W, Parr RG. Development of the Colle-Salvetti correlation-energy formula into a functional of the electron density. Phys Rev B 1988;37:785–789.
32. Francl MM, Pietro WJ, Hehre WJ, Binkley JS, Gordon MS, DeFrees DJ, Pople JA. Self-consistent molecular orbital methods. XXIII. A polarization-type basis set for second-row elements. J Chem Phys 1982; 77:3654–3665.
33. Hariharan PC, Pople JA. Influence of polarization functions on MO hydrogenation energies. Theo Chim Acta 1973;28:213–222.
34. Cossi M, Rega N, Scalmani G, Barone V. Energies, structures, and electronic properties of molecules in solution with the C-PCM solvation model. J Comput Chem 2003;24:669–681.
35. Olsson L, Cremer D. Prediction of nitrogen and oxygen NMR chemical shifts in organic compounds by density functional theory. J Phys Chem 1996;100:16881–16891.
36. Olsson L, Cremer D. Sum-over-states density functional perturbation theory: prediction of reliable 13C, 15N, and 17O nuclear magnetic resonance chemical shifts. J Chem Phys 1996;105:8995–9006.
37. Malkin VG, Malkina OL, Casida ME, Salahub DR. Nuclear magnetic resonance shielding tensors calculated with a sum-over-states density functional perturbation theory. J Am Chem Soc 1994;116:5898–5908.
38. Kraka E, Grafenstein J, Filatov M, Joo H, Izotov D, Gauss J, He Y, Wu A, Polo V, Olsson L, Konkoli Z, He Z, Cremer D. COLOGNE07. Stockton, CA: University of Pacific; 2007.
39. Sheldrick GM SHELXS-97. University of Gottingen, Germany; 1990.
40. Sheldrick GM SHELXL-97. University of Gottingen, Germany; 1997.